Zonal heterogeneity of peroxisome proliferation and morphology in rat liver after gemfibrozil treatment

K. Gorgas* **and S. K. Krisans[1]†**

Department of Anatomy and Cell Biology,* University of Heidelberg, Heidelberg, FRG, and Department of Biology and the Molecular Biology Institute,† San Diego State University, San Diego, CA 92182

Abstract The effect of gemfibrozil on the fine structure of peroxisomes across the rat liver lobule was investigated by light and electron microscopy using the alkaline diaminobenzidine (DAB) medium for the visualization of catalase peroxidatic activity. The oral administration of gemfibrozil for 2 weeks induces a striking heterogeneity in the lobular distribution of peroxisomes. The size and shape of peroxisomes, variety of matrix modifications, catalase content, and position within the cell, are functions of the zonal localization of the hepatocytes. The largest and most numerous peroxisomes were found in the centrilobular region indicating that these cells are most sensitive to peroxisome proliferation. On the other hand, the greatest variety of peroxisome shapes and matrix alterations (tubules and plates) was seen more peripherally in the mid-zonal and periportal regions. The larger, round centrilobular peroxisomes stained less intensely than the elongated peroxisomes found more peripherally, indicating a discrepancy between peroxisome size and catalase content. A distinct population of small irregularly shaped peroxisomes, lacking matrix specializations and containing variable catalase content, was found in the mid-zonal region. Peroxisomes in the centrilobular region were located within areas of the cell containing SER and glycogen while those in the more peripheral region were relegated to areas of the cytoplasm separate from RER and SER. In addition to modifications of peroxisomes, gemfibrozil treatment resulted in a proliferation and formation of whorled configurations of SER. This was particularly evident in the mid-zonal region, where single peroxisomal profiles could be seen surrounded by whorls of SER membranes. The results suggest that rat liver hepatocytes of the centrilobular region are the most sensitive to peroxisome proliferation and those of the periportal area are most susceptible to peroxisome matrix alterations after gemfibrozil treatment. —**Gorgas, K., and S. K. Krisans.** Zonal heterogeneity of peroxisome proliferation and morphology in rat liver after gemfibrozil treatment. *J. Lipid Res.* 1989. **30:** 1859–1875.

Supplementary key words diaminobenzidine • subcellular organelles • catalase

The peroxisome proliferative potency of structurally unrelated hypolipidemic drugs and industrial chemicals has been the subject of numerous biochemical and morphological investigations in the last decade using the liver of laboratory animals and nonhuman primates as a primary screening system (for review see refs. 1 and 2). Male rats demonstrate the most pronounced peroxisome response and therefore serve as sensitive test models for initial toxicological studies. In this species several morphological studies provide convincing evidence that potent peroxisome proliferators also induce a marked zonal heterogeneity of the peroxisome compartment across the liver lobule (3–5). Thus, in order to define the extent of peroxisome proliferation, the zonation within the liver lobule must be carefully taken into consideration.

It is well documented that gemfibrozil (Lopid) induces both an obvious proliferation of peroxisomes and a profound morphological alteration of the organelle matrix in the rat liver similar to other lipid-lowering agents classified as fibric acid derivatives. The matrix compartment has been shown to contain fibrillar inclusions in the form of plates and tubules, the latter often exceeding 4 μm in length (1, 6, 7). However, there is no information on the composition, function, and zone-dependent distribution pattern of these matrical inclusions.

The present study was designed to analyze the effects of gemfibrozil on the ultrastructural aspects of the rat liver lobule in detail with respect to peroxisome proliferation, zone-dependent distribution, and morphology. Special attention has been focused on the occurrence of fibrillar inclusions in the peroxisomal matrix in order to gain a better understanding of the zonal heterogeneity and plasticity of these cell organelles within the liver lobule.

Our data show that the effects of gemfibrozil on periportal cell layers differ considerably from those occurring within the centrilobular region. The area surrounding the afferent vessels (the terminal portal venule and the terminal hepatic arteriole) that is exposed to the highest concentration of substrates and oxygen within the liver lobule exhibits the most pronounced formation of matrical inclusions accompanied by a marked peroxisome elongation.

Abbreviations: DAB, diaminobenzidine.

[1]To whom correspondence should be addressed.

The region adjacent to the efferent vessel (the hepatic venule or central vein) shows a marked peroxisome proliferation and a significant enlargement in the organelle diameter, but only minor matrix alterations.

EXPERIMENTAL METHODS

Animals

Male Sprague-Dawley rats weighing 190–250 g were used in this study. A standard laboratory diet and lab chow supplemented with 0.2% gemfibrozil (Lopid, 5-(2, 5-dimethylphenoxy)-2,2-dimethylpentanoic acid, Warner–Lambert Company) were provided ad libitum for 14 days.

Perfusion fixation

Nonfasted animals were anesthetized with Vetalar (ketamine-HCl, 10 mg/100 g body weight) containing 0.1 mg acepromazine. This was followed by perfusion via the abdominal aorta, first with physiological saline containing 2.5% polyvinylpyrrolidone (PVP, 40,000 M. W.) for 15–30 sec followed by an ice-cold solution of 1.5% glutaraldehyde and 1.5% formaldehyde (freshly prepared from paraformaldehyde) in 0.1 M sodium phosphate (pH 7.6) containing 2.5% PVP for 5 min. The right liver lobes were excised immediately and 3-mm-thick tissue blocks were immersed in a freshly prepared fixative for an additional 15 min at 4°C.

Light and electron microscopy

Sections of 50–150 μm thickness were obtained either with an Oxford vibratome or razor blades and immersed in freshly prepared 2.5% glutaraldehyde solution in 0.1 M sodium cacodylate buffer (pH 7.6) containing 4% PVP and 0.05% calcium chloride for 10 min at 4°C. After rinsing in cacodylate buffer, the slices were postfixed for 60 min at 4°C in either a) 1% osmium tetroxide buffered with 0.1 M sodium cacodylate (pH 7.6), b) 1% osmium ferrocyanide (8), or c) a mixture of 1% osmium tetroxide and 2.5% potassium dichromate in 0.1 M cacodylate buffer. The samples were washed twice in cacodylate and 0.05 M maleate buffer (pH 5.2) and stained en bloc with 1% uranyl acetate in maleate buffer for 30–60 min at 4°C. The specimens were then dehydrated and embedded either in Epon 812 or in Araldite. Serial semithin sections of each specimen were used for orientation and examined either unstained or stained with Methylene Blue-Azur II (9). Central veins and portal triads were identified and serial ultrathin sections were stained with alkaline lead citrate for 30–60 sec (10) and analyzed in a Zeiss EM 10 electron microscope.

Cytochemistry

Catalase peroxidatic activity was visualized using the alkaline diaminobenzidine (DAB) medium of Le Hir et al. (11), consisting of 2 mg/ml of 3,3'-diaminobenzidine tetrahydrochloride (Merck, Sigma) and 0.15% hydrogen peroxide in 0.01 M Teorell-Stenhagen buffer at pH 10.0. The incubation was carried out for 15, 30, and 60 min at 37°C in a shaking waterbath. The shortest period of incubation was sufficient to obtain an adequate DAB staining which did not mask matrical inclusions and crystalline cores by reaction deposits.

Following incubation, selected thin tissue slices were postfixed in the above-mentioned osmium tetroxide solutions (a, b, c) and carefully processed for light and electron microscopy as described above.

RESULTS

Light microscopical findings

Gemfibrozil administration induces a pronounced peroxisome proliferation in the male rat liver as compared to controls (**Figs. 1a and 1b**). After visualization of the catalase peroxidatic activity with the alkaline DAB-medium, an analysis of the peroxisomal compartment within the liver lobule reveals a stepwise numerical increase of peroxisomes per hepatocyte from the periportal towards the centrilobular region which coincides with gradual changes in organelle size, shape, and catalase content. The highest density of peroxisomal profiles is always found in cell layers adjacent to

Fig. 1. Light micrographs of the male rat liver treated for 2 weeks with gemfibrozil (a, c–f) and control liver (b). Unstained semithin Araldite sections (0.75 μm) incubated in the alkaline diaminobenzidine medium (DAB) for the visualization of the catalase peroxidatic activity (a, c–f: DAB-buffered osmium tetroxide; b: DAB-reduced osmium tetroxide). a) A remarkable shift in peroxisome density and diameter from the periportal towards the centrilobular area is clearly seen. Giant and round peroxisomes are most abundant in the cell layer adjacent to the central vein. The areas marked with rectangles are enlarged in figures d, e, and f. × 205. b) Control liver hepatocytes of the periportal region display few peroxisomes when compared to those of gemfibrozil treated rats (c and d). In the centrilobular zone (data not shown) the number of peroxisomes differs only slightly from that in the periportal area. × 1200. c) In a limited number of rats treated with gemfibrozil, hepatocytes of the periportal cell layers contain only a few needle-like peroxisomes (compare with d). ibd-interlobular duct. × 1200. d) The periportal zone of the liver lobule exposed to gemfibrozil is normally characterized by numerous thin needle- or rod-shaped peroxisomes lining large glycogen areas (large arrowhead); tpiv, inlet venule of the terminal portal venule; small arrowhead, nucleus of a fat-storing cell. × 1200. e) The highest frequency of both typical phi-bodies with long protrusions (small arrowhead) and prominent, well-developed SER-whorls is found in the outer midzonal region of the liver lobule. The latter appear as moderate electron-dense, ring-like structures which often enclose peroxisomes (large arrowhead); cv, central vein. × 1200. f) In the centrilobular region only a few phi-bodies with one or two short and thin projections (arrowhead) are intermingled within the huge population of round peroxisomes which occupy large areas of the cytoplasm. × 1200. Bars, (a) 100 μm, (b)-(f) 10 μm.

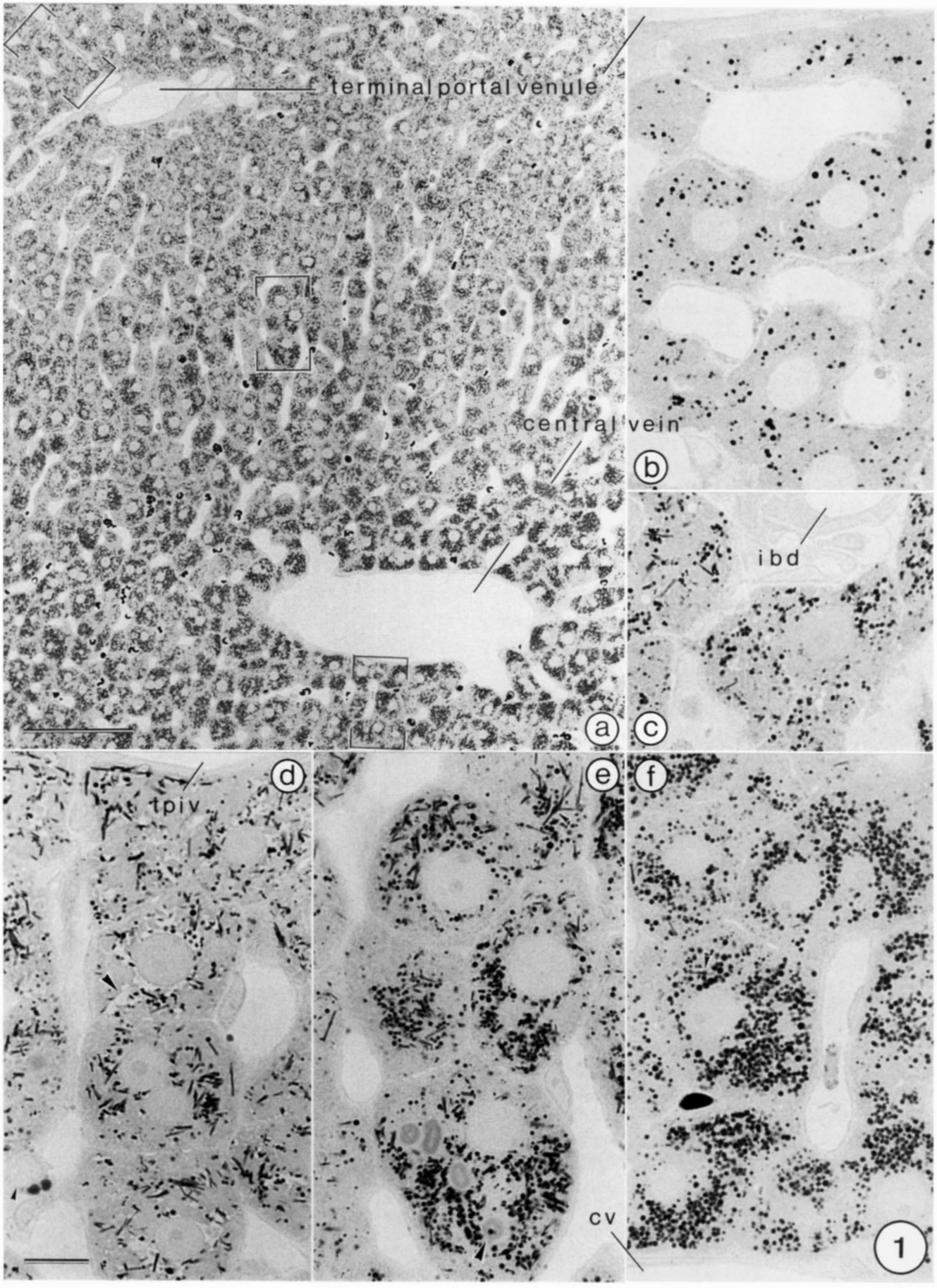

the central vein (Figs. 1a and 1f), whereas the greatest frequency of thin needle- and rod-shaped organelles exceeding 10 μm in length is seen in the periportal area (Fig. 1d). The number of so-called phi-bodies, peroxisomal profiles that exhibit a large round or elliptical central portion and two long axial protrusions, is greatest in the outer midzonal region (Fig. 1e). They can reach a length of up to 12.5 μm. Phi-bodies with short projections and a length of approximately 4 μm are characteristic for the inner midzonal region. Their number decreases remarkably towards the outer centrilobular region, and in hepatocytes of the perivenous limiting plate, one or two mostly racket-shaped peroxisomes equipped with only one thin process occur. Thus, the inner centrilobular cell layers contain a uniform peroxisomal population comprised almost exclusively of round particles with a large mean diameter and a slightly decreased catalase activity (Fig. 1f).

A remarkable variation among the treated animals is observed in the number of needle-like peroxisomes and phi-bodies. In a limited number of rats, these atypical organelles are comparatively sparse and confined to the outer lobular regions (compare Figs. 1d with 1c).

In addition to the peroxisome proliferation, moderately electron-dense ring-like structures appear within the cells, often enclosing one to three peroxisomes (Fig. 1e, arrowhead). Such whorls of SER appear to be randomly distributed in the periportal limiting plate as well as throughout the outer periportal area. However, in the inner periportal region, a remarkable increase in size and frequency of these SER-lamellar bodies can be demonstrated. They are most abundant and best developed in the outer midzonal region. In the inner midzonal region the SER-lamellar bodies decrease remarkably in number and size, and in the centrilobular zone these concentrically arranged membrane aggregates are rarely observed.

Electron microscopical findings

The fine structural analysis of the liver lobule of gemfibrozil-treated rats reveals marked morphological alterations in the peroxisome and endoplasmic reticulum compartments and less extensive changes in mitochondria and lysosomes (data not shown) as well as in the nuclear matrix.

Morphology of peroxisomes

Across the liver lobule, peroxisomes exhibit a conspicuous zonal heterogeneity not only in their number, shape, and length as seen in light microscopy, but also with respect to their diameter, catalase content, and intracellular compartmentation. In addition, a marked gradient of matrical inclusions, small peroxisomal profiles, and organelle stacking patterns from the periportal towards the centrilobular region is observed.

Diameter, catalase activity and intracellular distribution. Hepatocytes of the periportal limiting plate contain intensely stained, needle- and rod-shaped peroxisomes that appear round to oval with a characteristic scalloped outline in cross sections (**Fig. 2a**). They exhibit a diameter between 25–750 nm with a mean of 350 nm, the majority ranging from 200 to 500 nm. The organelles are mostly located at the periphery of small glycogen areas facing cytoplasmic regions which consist of stacks of parallel cisternae of rough endoplasmic reticulum (RER) and large mictochondria.

In typical periportal hepatocytes, the needle- and rod-shaped peroxisomes often occur in clusters. The strongly DAB-positive organelles display a wavy appearance of their limiting membrane (Fig. 2b and **Fig. 3**) and exhibit a mean diameter of 375 nm. They line not only large glycogen areas, but also tend to encase aggregates of anastomosing profiles of smooth endoplasmic reticulum (SER) not seen in control animals. RER-stacks increased in number as compared to controls, and radiating individual smooth cisternae partially or completely surround mitochondria as well as peroxisomes.

In hepatocytes of the midzonal region, peroxisomes undergo striking proliferation and display marked heterogeneity with respect to their size, shape, and amount of reaction deposit (Figs. 2c, 4, 5a, d). They range from 25 to 1050 nm in diameter with a mean of 475 nm exhibiting two peaks: *a*) 250–500 and *b*) 500–800 nm. The majority of peroxisomes show distinct but less intense DAB-staining when compared to those of periportal cells. In addition to round organelles, numerous phi-bodies and irregularly shaped particles are observed (**Fig. 4**). They are all densely packed and occupy distinct cytoplasmic areas separated from those containing RER-stacks and SER-membrane aggregates.

A marked variation in peroxisome size and DAB-staining intensity is also seen in centrilobular cells. However, in this region peroxisomes show a moderate amount of DAB reaction deposit, a preferential round shape, and an almost even

Fig. 2. Low power electron micrographs of the male rat liver treated for 2 weeks with gemfibrozil. DAB-buffered osmium tetroxide containing 2.5% potassium dichromate. × 6200. a) Hepatocytes of the periportal limiting plate display small intensely stained peroxisomes which show a scalloped outline and preferentially face small glycogen areas. In the latter a few electron-lucent (L) or moderately osmiophilic lipid droplets (arrowheads) can be observed. b) In the typical periportal liver cells, strongly DAB-positive peroxisomes appear in clusters which line and extend towards large glycogen areas. Note the abundance of anastomosing tubular profiles of smooth endoplasmic reticulum (SER) at the cell periphery. The arrow designates a racket-shaped peroxisome. L and arrowhead, electron-lucent and moderately osmiophilic lipid droplets. c) In the outer midzonal region enlarged, moderate to intensely stained peroxisomes accumulate in distinct cytoplasmic areas which are separated from those consisting of RER-arrays or SER-membrane aggregates (SER, SER-whorl large arrowhead). The peroxisomes exhibit a specific close association with one another (small arrowheads). d) Peroxisomes exhibiting the largest diameters are found in the perivenous limiting plate. They preferentially appear round and the majority contain comparatively moderate amounts of reaction deposit. Although most organelles are evenly distributed throughout the SER-areas, a few cluster in chain-like arrangements (small arrowheads). A limited number of peroxisomes contain matrical inclusions (large arrowheads). Bar, 3 μm.

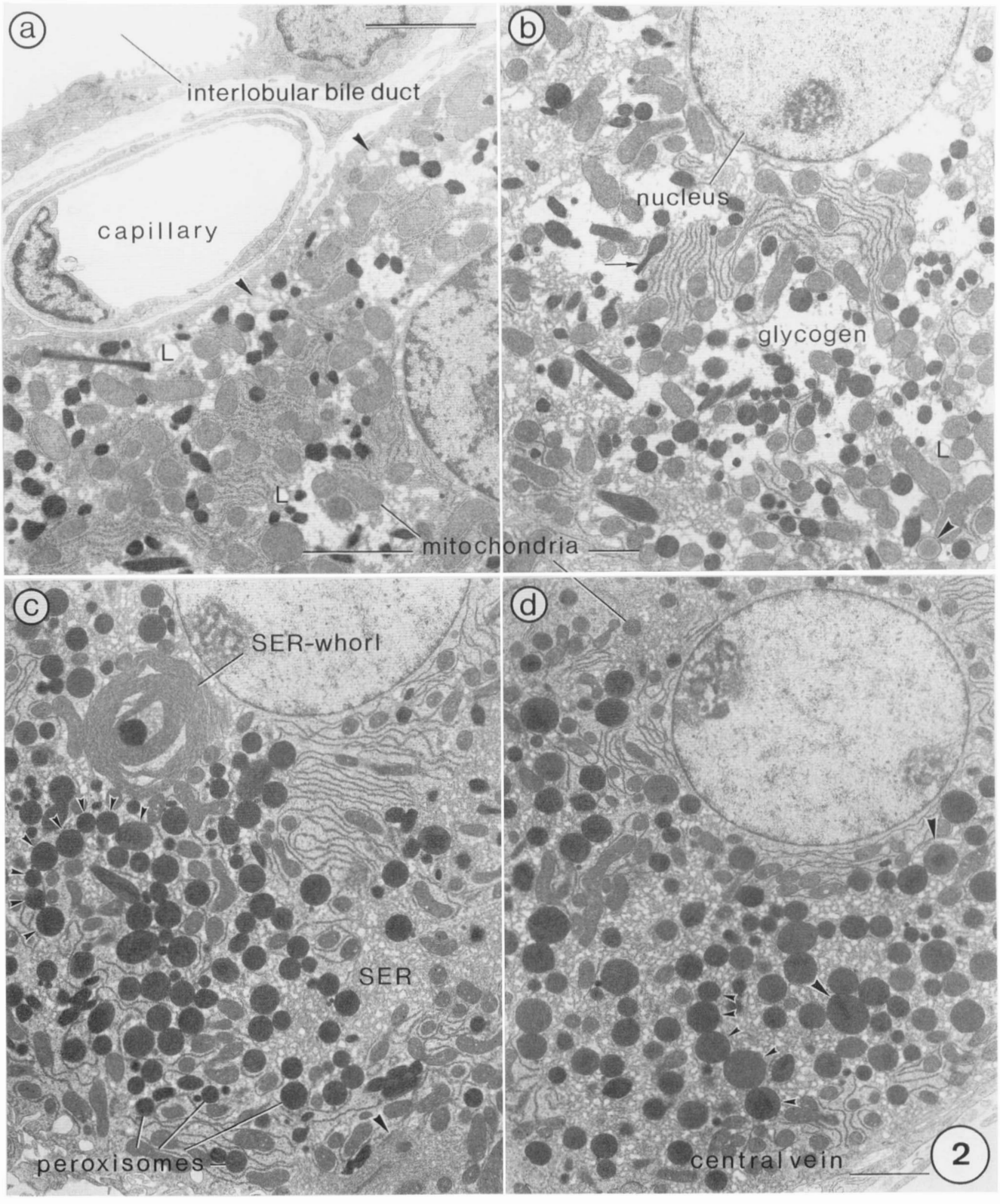

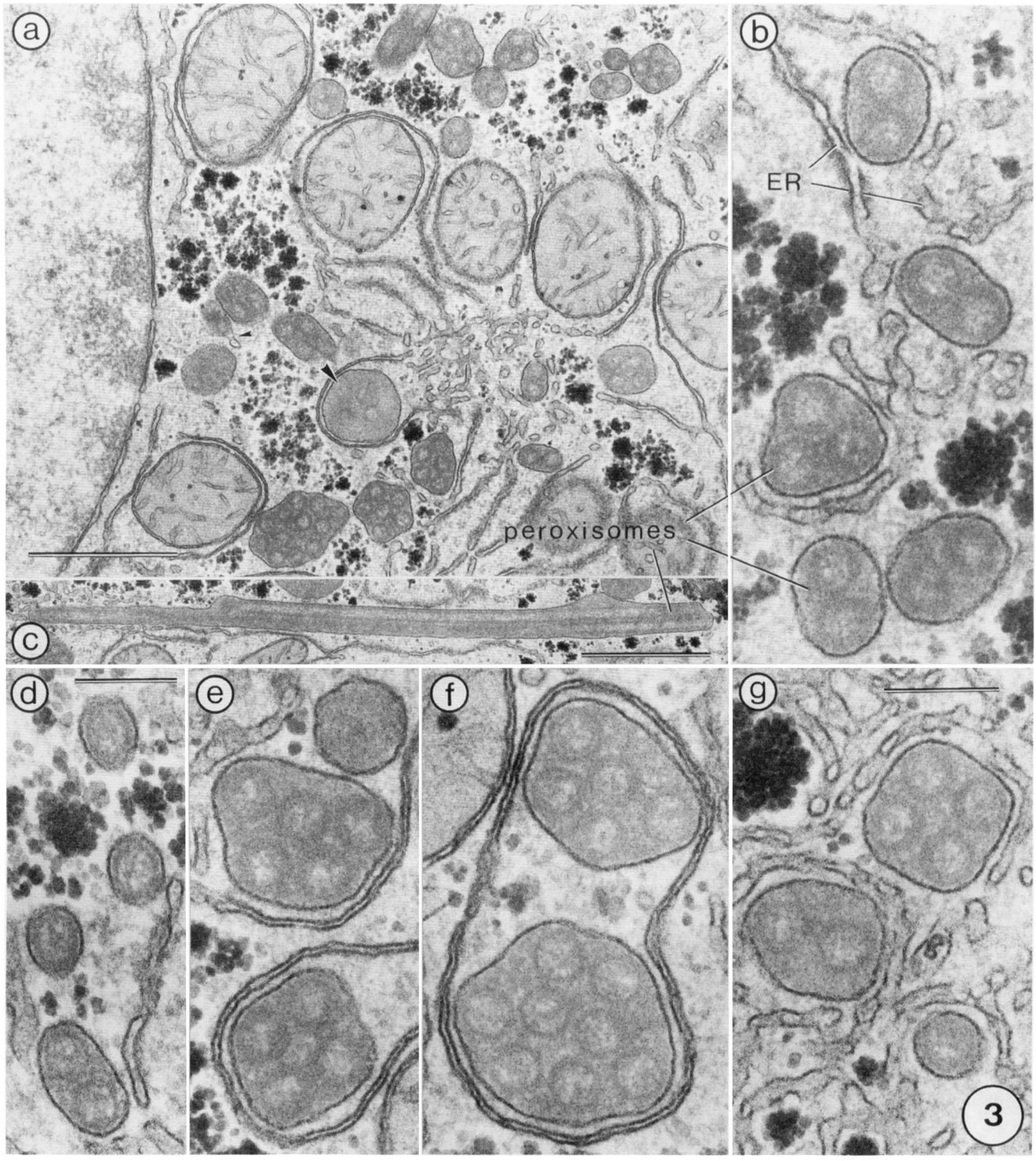

Fig. 3. Electron micrographs of periportal hepatocytes of the male rat liver 2 weeks after gemfibrozil treatment. Short DAB-incubation (15 min)-reduced osmium tetroxide. a) In periportal hepatocytes the majority of peroxisomal profiles contain one to four matrical tubules, the latter of which exhibit only weak catalase activity in their lumen. Note a tubule-containing peroxisome with a tail-like extension lacking catalase activity (small arrowhead). Large arrowhead, nucleoid-containing peroxisomal profile. × 25,500. b) and d) In periportal hepatocytes the dimensions of the cross-sectioned peroxisomes correlate with the number of enclosed straight tubules. The organelles display an intimate spatial relationship to profiles of the endoplasmic reticulum (ER) and glycogen particles. b) × 80,000; d) × 69,500. c) Needle- and rod-shaped peroxisomal profiles equipped with longitudinally arranged matrical tubules are characteristic for hepatocytes of the periportal zone. × 22,000. e) and f) In hepatocytes of the inner periportal zone peroxisomal profiles containing more than four matrical tubules are often partially or completely surrounded by nonfenestrated SER-cisternae. Organelles ranging from 145 to 200 nm in diameter normally contain one matrical tubule. Occasionally, the latter may also be absent (compare the peroxisomal profile in the upper right corner in (e) with those in (d) or that in the lower right corner in (g)). × 80,000. g) Towards the inner periportal zone, the thin, tube-like portions of the rod-shaped peroxisomes which exhibit mostly less than four matrical tubules are enmeshed by an anastomosing network of SER-profiles. × 80,000. Bars, (a) (c) 1 μm, (b)–(g) 250 nm.

distribution throughout the glycogen-SER areas. In some hepatocytes the SER-regions are completely devoid of glycogen. The peroxisomal profiles display a mean diameter of 630 nm, most ranging from 500 to 800 nm. In hepatocytes of the perivenous limiting plate, a number of large peroxisomes exceeding a diameter of 1200 nm are present (Fig. 2d).

Peroxisomes and mitochondria in hepatocytes of the periportal and perivenous limiting plate show a marked inverse relationship with respect to their diameters (compare Fig. 2a with 2d). Periportal liver cells contain remarkably large mitochondria and small peroxisomal profiles, whereas the opposite is true for centrilobular hepatocytes. Furthermore, a marked alteration in the pattern of organelle distribution is evident. In periportal hepatocytes a compartmentation of peroxisomes with mitochondria and RER-cisternae can be observed, whereas in the centrilobular cells peroxisomes exhibit a close spatial relationship to the SER-profiles.

Matrical inclusions. Following gemfibrozil treatment, peroxisomes exhibit a well-developed crystalline core and either distinct straight matrical tubules or curled matrical plates, the presence and number of which differ greatly depending on the localization of hepatocytes within the liver lobule.

In the majority of treated rats, representative of the periportal zone are peroxisomes containing exclusively densely packed double-walled matrical tubules (Fig. 3a). The tubules are aligned in parallel along the major axis of the needle- and rod-shaped organelles separated from the limiting membrane by a narrow space of 10–12.5 nm in width (Figs. 3e–g). The peroxisomal profiles exhibit a scalloped or wavy contour in cross sections (Figs. 2a, b; 3a, b, e–g), whereas a regular rectangular shape is seen in longitudinal sections. The tubule length may vary considerably creating the typical staircase-like conformation in the majority of organelles (Fig. 3c). Therefore, in cross sections the number of matrical tubules, even within a single organelle, may range from 1 to 12 (Figs. 3a, b, d–g).

The dimensions and fine structure of the matrical tubules resemble those described in detail by Hruban and coworkers (12) in rat liver treated with dimethrin. The tubular structures exhibit a uniform outer diameter of 112.5 nm. They consist of an outer and an inner tubule composed of helically arranged fibrils (Fig. 4C). The catalase activity appears to be concentrated between the fibrils, whereas the lumen of the double-walled tubules displays variable DAB-staining (compare Figs. 2a–d and Fig. 7b: 60 min DAB-incubation with Figs. 3 a–g and 4 a, b, d–g: 15 min DAB-incubation).

In hepatocytes of the midzonal region, peroxisomes exhibit an abundance of matrical tubules or matrical plates, with tubules predominating in peripheral cells and plates being most prominent in more centrally located cells of this region (Fig. 4a). Among the tubule-containing peroxisomes, a marked variation in shape is observed based on the number, length, and arrangement of the double-walled inclusions. A preponderance of typical phi-bodies is seen in the outer midzonal region (Figs. 4b, d) and irregular, discoid, and racket-shaped organelles are representative of the inner midzonal area (Figs. 4f–h).

In agreement with light microscopical findings, typical phi-bodies exhibit an enlarged round to elliptical central portion of variable size and two long axial protrusions which often display the same length and diameter (Figs. 4b, d). The double-walled tubules are usually oriented in parallel and extend from pole to pole tightly attached to the membrane apex (Fig. 4d). Cross sections of the dilated portions of phi-bodies can easily be identified as large round to oval profiles frequently containing more than a dozen of densely packed, centrally located matrical tubules separated from the limiting membrane by a distance exceeding at least 20 nm in width (Figs. 4a, e, and **Fig. 5e**). In contrast, cross sections of the tube-like, straight axial protrusions exhibit a wavy outline and contain mostly 1–4 matrical tubules closely attached to the peroxisomal membrane (Figs. 4a, b, e).

Several phi-bodies exhibit protrusions which are not aligned along the major axis but form an angle of 145° or less. Thus, matrical tubules traverse in the central dilated portion (Fig. 4b) and cross sections of the latter exhibit densely packed groups of matrical tubules distinctly separated from each other (Fig. 4a, large arrowhead). Occasionally, enlarged pleomorphic organelles are found containing bundles of matrical tubules running in various directions, such that transverse, oblique, and longtitudinal sections of as many as 20 tubules may be present within the same organelle (Figs. 4f, g).

Towards the centrilobular region, double-walled tubules within the hepatocytes decrease considerably in number and length. However, even in the perivenous limiting plate the majority of gemfibrozil-treated rats develop a small population of spindle-shaped phi-bodies with short protrusions as well as discoid and racket-shaped organelles. The latter are composed of elliptical dilated portions and thin, single tubule-containing protrusions radiating into the SER-glycogen areas (Fig. 4h).

In the majority of treated rats the formation of matrical plates is most prominent in the midzonal region (Figs. 4a, b, e). Concomitant with the decrease of tubule-containing peroxisomes, the percentage of profiles exhibiting matrical plates within a hepatocyte increases. However, in the inner centrilobular region the number of matrical plates is remarkably reduced (**Fig. 6c**) and in the perivenous limiting plate only a few organelles displaying these inclusions can be identified. In a limited number of treated rats matrical plates are rare throughout the liver lobule. The fine structure of the matrical plates is identical to those previously reported by Hruban and coworkers (12) in the rat liver

treated with dimethrin. The fibrillar plates form a loose network of small curled or slightly bent inclusions which following DAB-incubation appear as irregularly shaped, filamentous densities located mainly in the centre of the peroxisomal matrix (Figs. 3a, b, e, 6c). Thus, the reaction deposit obscures their fibrillar organization as similarly seen within matrical tubules.

Crystalline nucleoids are regularly encountered in peroxisomes of the periportal region. They are displaced towards the periphery of the elongated organelles lying between the limiting membrane and the double-walled tubules creating slight local protusions. With respect to the organelle length only a few round peroxisomal profiles in cross section contain a crystalline core (Fig. 3a, large arrowhead). In the midzonal region nucleoids can easily be identified. They are exclusively located in the enlarged central portions of phi-bodies as well as in peroxisomes containing matrical plates (Figs. 4b, d–f, 5e). In random thin sections the highest frequency of nucleoids is observed in the centrilobular region.

Small peroxisomal profiles. The most prominent population of small peroxisomal profiles can be demonstrated in hepatocytes of the inner midzonal region (Figs. 5a, f). The organelles range from 25 to 175 nm in diameter and never contain matrical inclusions. They exhibit a weak to intense DAB-staining depending on their size. The majority are located in close proximity to large, strongly DAB-reactive organelles and intimately related to terminal portions of RER-stacks and SER-membrane aggregates (Figs. 5a, b, f). They often occur in clusters forming rows and beaded strings (Figs. 5a, c). In appropriate planes of sections, branching sites of tubular organelles (Fig. 5a, inset) as well as interconnections between peroxisomal profiles of different sizes are frequently observed (Figs. 5b, c, f, 6d). These short and thin channels (25–50 nm in diameter) exhibit a patchy distribution of reaction deposit or totally lack catalase activity. Thus, in cross sections the channels are confusingly similar to vesicular SER-profiles and can be unequivocally identified only in serial sections (Fig. 5c, large arrowhead). The same is true for numerous slender, tail-like extensions which occur throughout the liver lobule but are most abundant in the midzonal region (Figs. 3a, 5d, f). Their terminal membrane portions often exhibit a myelin-like appearance (Fig. 4e). In cross section, this criterion helps to define the origin of these vesicles and estimate the number of 'tails' per hepatocyte in random thin sections.

Stacking of peroxisomes. Another feature observed in hepatocytes of the male rat liver exposed to gemfibrozil is the development of a distinct stacking or packing pattern of peroxisomes. A gradual increase in the dense packing of peroxisomes can be demonstrated from the periportal towards the centrilobular region which is most pronounced in the inner midzonal and outer centrilobular region (Figs. 2c, d, 6a, c). In random thin sections, as many as 12 organelles with or without matrical inclusions are stacked one upon the other forming undulating rouleau- or chain-like structures. The organelles are closely apposed and constitute straight and parallel, junction-like contact zones of considerable length (Figs. 6a–d). Occasionally, small peroxisomal profiles bulge into larger ones (Fig. 6d). Numerous fine filaments traverse the intermembraneous space (8–9 nm) in the region of the most intimate membrane contact. They appear to insert into the outer membrane leaflets linking the two adjacent membrane faces (Fig. 6b).

Membrane aggregates of smooth endoplasmic reticulum

The smooth endoplasmic reticulum undergoes a marked proliferation from the periportal towards the centrilobular region, (compare Figs. 2a, b with c, d). In addition, lamellar cisternae as well as branching and anastomosing tubules constitute large membrane aggregates which display a zone-dependent variation with respect to size, organization, and degree of complexity.

Two types of concentric lamellar formations can be distinguished mainly ranging from 1 to 10 μm in diameter: myelin-like bodies and fingerprint-whorls. The myelin-like bodies are preferentially located adjacent to the nucleus and consist of 3–30 paired layers of densely packed, nonfenestrated SER-cisternae. They are arranged in parallel arrays and often surround a core of variable size which may contain lipid droplets, liposomes (located within dilated cister-

Fig. 4. Electron micrographs of hepatocytes of the midzonal region of the male rat liver treated for 2 weeks with gemfibrozil. a), b), d–g): short DAB-incubation-reduced osmium tetroxide, c): buffered osmium tetroxide, h): reduced osmium tetroxide. a) Low power electron micrograph of a typical midzonal hepatocyte showing numerous enlarged peroxisomal profiles which contain either densely packed matrical tubules or curled matrical plates in their centre. Infrequently, the tubules are arranged in groups distinctly separated from each other (arrowhead). RER, stack of rough endoplasmic reticulum. × 13,000. b) A phi-body with two protrusions forming an angle of 145°. A nonfenestrated ER-cisterna is closely related to the elliptical central body of the organelle. SER, network of smooth endoplasmic reticulum; arrowhead, crystalline nucleoid. × 19,000. c) The fibrillar structure of the double-walled matrical tubules is clearly visible. The crystalline nucleoid is mostly eccentrically located. × 66,000. d) A typical phi-body with two long protrusions of approximately the same length displays matrical tubules which are arranged in parallel throughout the long axis of the central elliptical region. Arrowhead, crystalline nucleoid. × 15,000. e) Independent of organelle size and type of matrical inclusions (plates or tubules), peroxisomes exhibit a great variation in DAB-staining intensity. A few display only small amounts of reaction deposit and the crystalline nucleoid (large arrowhead) is easily recognizable (compare with g–d and f). Small arrowhead, tail-like extension exhibiting a modified membrane structure at the apex. × 42,000. f) Enlarged polymorphic peroxisomes display numerous matrical tubules which run in different directions. Arrowhead, crystalline nucleoid. × 33,000. g) A Y-shaped peroxisome is filled with matrical tubules radiating into the protrusions. Note the closely attached nonfenestrated ER-cisternae on both sides of the central organelle region. × 33,000. h) A racket-shaped peroxisome located in the inner midzonal region displays only one matrical tubule. The elongated protrusion exhibits contact zones at the distal portion to three adjacent peroxisomal profiles. Arrowhead, cross section of a thin, one tubule-containing protrusion. × 33,000. Bars, (a) (b) (d) 1 μm, (c) (e) 250 nm, (f)–(h) 500 nm.

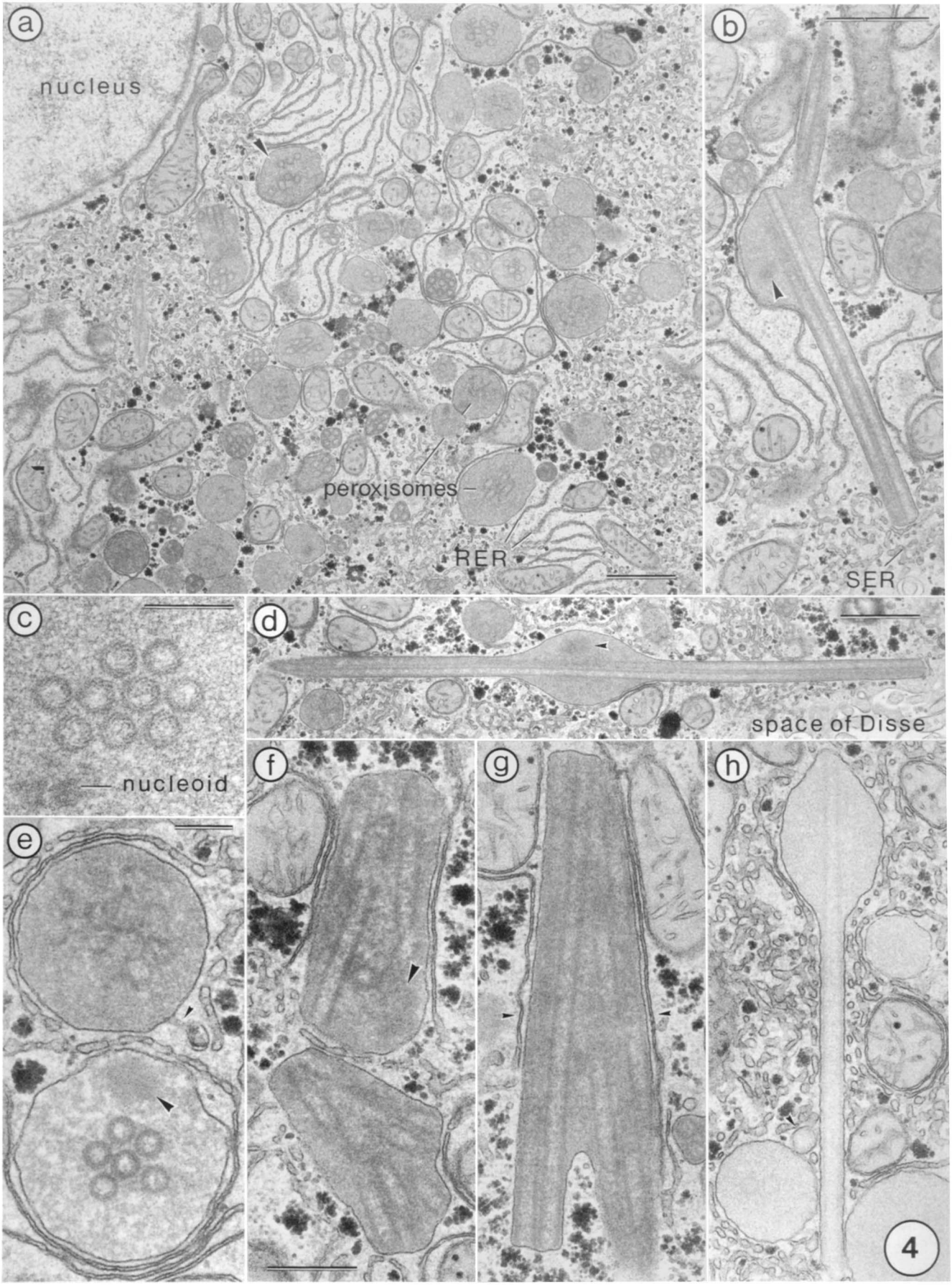

nae), a few mitochondria and lysosomes as well as peroxisomes (Figs. 1e, 2c). The paired membranes display a compact stacking in the inner layers and thus appear in light microscopy as moderately stained ring-like structures (Fig. 1e). A variable number of peripheral paired lamellae radiate into the cytoplasm and form small stacks of variable length frequently in the vicinity of the perinuclear cisterna (Fig. 2c).

Myelin-like bodies exhibiting a limited number of paired lamellae occasionally occur in hepatocytes of the periportal limiting plate. Their number and size remarkably increase towards the midzonal region. In random thin sections hepatocytes of the outer midzonal area frequently contain 3–4 large myelin-like bodies consisting of 15–30 paired lamellae encasing distinct cytoplasmic portions. Concomitant with the decrease of myelin-like bodies towards the inner lobular regions, fingerprint-whorls increase proportionately. The latter are composed of 20–50 concentrically arranged, irregularly fenestrated cisternae (Fig. 5e). Both the inter- and intra-cisternal spacing as well as the concentric organization of the layers are relatively uniform and regular throughout the aggregate. The central cisterna is often nonfenestrated and surrounds cell organelles, such as mitochondria or peroxisomes, without an intervening cytoplasmic strand (Fig. 5e). Fingerprint-whorls rarely occur in the outer periportal and inner centrilobular cell layers. They are most abundant in the midzonal region.

Branching and anastomosing SER-tubules form loose membrane systems in all hepatocytes of the liver lobule. However, their extent markedly increases towards the midzonal and centrilobular regions (compare Fig. 3a with Figs. 4a, 5a, and 6a). In addition, dense packing of branching tubular SER-profiles and formation of large membrane aggregates mostly occurs in the inner midzonal and outer centrilobular regions (Fig. 5f).

Changes in the nuclear structure

Gemfibrozil treatment induces morphological alterations in the nuclear structure of hepatocytes and elicits the mitogenic potency of this drug in male rat liver.

Nuclear lipid inclusions. An increase in the number of small lipid droplets regularly encountered in the periportal and outer midzonal hepatocytes (Figs. 2a, b and **Fig. 7b**) parallels the occurrence of intranuclear lipid inclusions in corresponding cell layers. In random thin sections nuclei contain a variable number of lipid droplets (1–4) which often closely approximates the nucleolus (Fig 7b) but not the nuclear envelope. The inclusions range from 500 to 1200 nm in diameter. They are enveloped by a thin electron-dense lipid leaflet followed by a distinct zone measuring up to 175 nm in width. The latter displays a regular filamentous texture clearly distinguishable from the chromatin-containing regions, the finely granular nuclear matrix and the nucleolus (Fig. 7c, arrowheads).

Cell division. Gemfibrozil induces a pronounced liver cell proliferation as demonstrated by an increased number of mitotic figures, predominantly within the midzonal region. In contrast to controls, various stages of the mitotic cycle can easily be demonstrated (Fig. 7a). It is of interest that the stacking of peroxisomes typical for the organelle compartment in hepatocytes of the midzonal region is not expressed in mitotic liver cells.

DISCUSSION

The findings presented in this study demonstrate that gemfibrozil treatment of male rats results in significant morphological alterations in the liver: *1*) peroxisome proliferation as demonstrated by both a remarkable increase in organelle number and size; and *2*) proliferation of smooth endoplasmic reticulum. These results are consistent with previous fine structural studies of the rat liver exposed to gemfibrozil and to a variety of other compounds, structurally related as well as unrelated (for review see 1, 2, 13, 14). In addition to these well-characterized hepatic responses, our observations also reveal that gemfibrozil elicits a cascade of subcellular changes not as yet described. The most marked effects include *A*) a conspicuous zonal heterogeneity in per-

Fig. 5. Electron micrographs of hepatocytes of the inner midzonal region of the male rat liver 2 weeks after gemfibrozil administration. a) A characteristic feature of the inner midzonal hepatocyte is the remarkable heterogeneous peroxisomal population with respect to size and amount of reaction deposit. Small peroxisomal profiles never contain matrical tubules and frequently occur in clusters (large arrowheads) or in tightly packed rows (small arrowheads). lys, lysosomes; mit, mitochondria. DAB-buffered osmium tetroxide containing 2.5% potassium dichromate. × 19,500. Inset: Branching peroxisomal profiles frequently occur (arrowhead). DAB-reduced osmium tetroxide. × 20,000. b) Small peroxisomal profiles (small arrowhead) often appear in close proximity to large intensely stained organelles and exhibit a patchy distribution of reaction deposits. The short interconnecting channels between peroxisomal segments display very weak catalase activity (large arrowhead). DAB-buffered osmium tetroxide containing 2.5% potassium dichromate. × 62,500. c) Beaded strings with more than three strongly DAB-positive peroxisomal segments are frequently observed. The thin interconnecting channels (small arrowheads) often lack catalase activity and in cross sections resemble adjacent SER-vesicles (large arrowhead). DAB-buffered osmium tetroxide containing 2.5% potassium dichromate. × 62,000. d) The central region of a phi-body with short axial protrusions is equipped with a tail-like extension. The transition zone is demarcated by a slight constriction (large arrowhead). Reduced osmium tetroxide. × 38,750. e) The central region of a phi-body with densely packed matrical tubules and an eccentrically located crystalline core (small arrowhead) is enveloped by a nonfenestrated cisterna followed by more than a dozen of irregularly fenestrated SER-lamellae forming a whorl. Short DAB-incubation-reduced osmium tetroxide. × 19,500. f) Towards the centrilobular region, densely packed anastomosing tubular SER-profiles form large membrane aggregates which are surrounded by peroxisomes and mitochondria. In the latter, dilated cristae are occasionally identified (asterisk) containing helically arranged filaments in a paracrystalline array (not shown). Large arrowheads, clusters of small peroxisomal profiles; small arrowheads, a nucleoid-containing peroxisomal profile connected to a small tubular segment; RER, cisternae of rough endoplasmic reticulum. Short DAB-incubation-reduced osmium tetroxide. × 19,500. Bars, (a) (e) (f) 500 nm, (b) (c) (d) 250 nm.

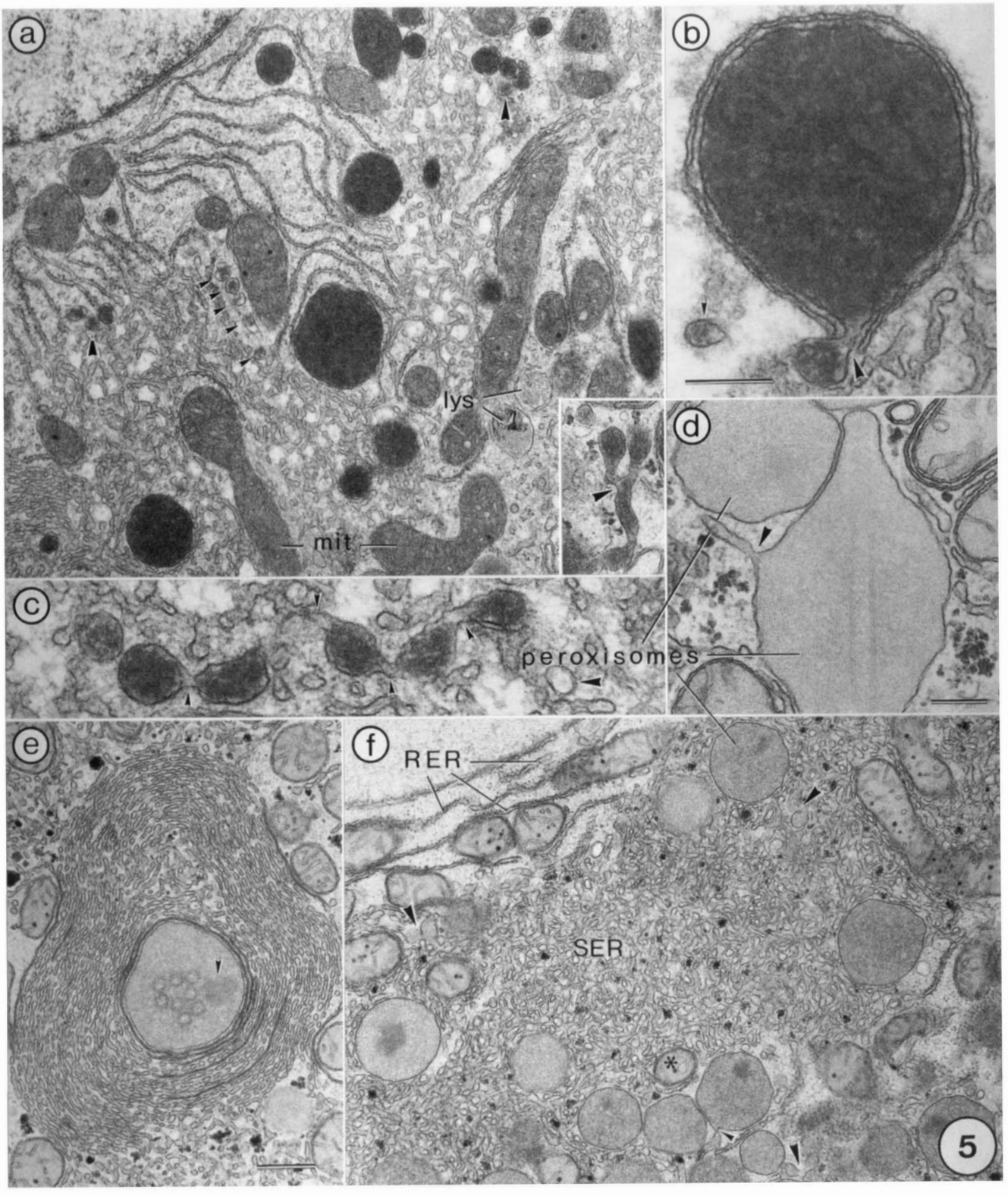

oxisome proliferation and morphology, *B*) a lobular gradient in peroxisome stacking, *C*) the formation of myelin-like bodies and fingerprint-whorls of smooth endoplasmic reticulum, and *D*) the occurrence of nuclear lipid inclusions.

Zonal heterogeneity

Peroxisome proliferation and catalase activity. In all rats treated with gemfibrozil a remarkable zone-dependent shift in the peroxisome number, size, and catalase activity from the periportal to the centrilobular regions can be observed. These zonal differences in the peroxisomal organization after gemfibrozil treatment are comparable to those previously described in the rat liver after treatment with perfluorooctanoate (5). Earlier observations demonstrated a larger number of peroxisomes in the more centrally located cells of the normal rat liver lobule (15, 16). Our data support the concept that potent peroxisome proliferators markedly enhance the zonal heterogeneity of the peroxisomal compartment and exert the greatest proliferating potency in the centrilobular region (for detailed discussion see 5).

In human liver, gemfibrozil and various other fibric acid derivatives are reported to elicit marginal or no peroxisome proliferation (for review see refs. 1 and 2). The marked variation in peroxisome number and volume densities described in human liver after gemfibrozil exposure (17, 18) and the significant increase in peroxisome number in patients after long-term clofibrate treatment (19, 20) should not be overlooked. The increased clinical use of lipid-lowering compounds for the effective control of hyperlipoproteinemias may deem it necessary to reinvestigate human liver biopsies with special reference to alterations of the peroxisomal compartment in the centrilobular region to assess potential human health and cancer risk. It is noteworthy, however, that results from the Helsinki Heart Study using gemfibrozil showed a 34% reduction in cardiac end point compared to placebo with no clinically significant adverse events involving liver function (21).

Our results also reveal that there is a disparity between peroxisome volume and the intensity of DAB reactivity across the liver lobule. High levels of cytochemically demonstrable catalase activity are confined to the smaller organelles in the periportal region whereas the large peroxisomes found in the inner cells stained only moderately. The decrease in DAB reaction deposit coincides with a marked increase in the number of peroxisomes per cell. Our observations are consistent with data showing that treatment with peroxisome proliferators does not result in an elevation of catalase activity proportional to the increase in peroxisome volume. (For review see refs. 1, 22, 23).

Matrical inclusions. Double-walled tubules. Our observations confirm earlier reports that double-walled tubules with a uniform diameter of approximately 100 nm represent typical inclusions of the peroxisomal compartment in the rat liver after exposure to gemfibrozil (1, 6, 7, 24). Identical or similar double-walled inclusions have been described in rat liver peroxisomes after treatment with various structurally related and diverse drugs. However, a high frequency of double-walled inclusions seems to be easily induced only in response to gemfibrozil, dimethrin (12, 25), and RMI-14, 514 (26), whereas clofibrate, bezafibrate, and aspirin exclusively elicit these specific alterations in the peroxisome matrix after severe metabolic stress situations, for example hypophysectomy (27), long-term and high dosage treatment (28), or additional exposure to hepatocarcinogens (29–32). Furthermore, corresponding tubular inclusions have also been reported in peroxisomes of very slow-growing Morris 7787 hepatoma cells (33, 34) as well as in highly differentiated hepatomas treated with clofibrate (30). As yet, the composition and functional significance of these matrical inclusions are unknown. It is interesting to note that rat kidney peroxisomes in the proximal tubule (P3-segment) normally exhibit both tubular inclusions with a crystalline substructure (35–37) and a specific distribution pattern of matrix proteins as demonstrated by cytochemistry and immunoelectron microscopy. Catalase, L-α-hydroxy acid oxidase, and serine:pyruvate aminotransferase as well as the β-oxidation enzymes are found to be preferentially located in the peripheral matrix portions dispersed between the tubular structures. In contrast, D-amino acid oxidase is exclusively confined to the central matrix area (38, 39).

Matrical plates. Our observations confirm findings reported by Fukuda and coworkers (6) that gemfibrozil induces the formation of matrical plates within the peroxisome matrix in addition to the development of tubular inclusions. However, the distribution pattern of matrical plates differs markedly from that of matrical tubules. The greatest concentration of plate-containing peroxisomes is regularly found in the midzonal and outer centrilobular regions. Similar structures have previously been described in peroxisomes of rat liver exposed to a variety of drugs and experi-

Fig. 6. Electron micrographs of centrilobular hepatocytes of the male rat liver 2 weeks after gemfibrozil administraton. Short DAB-incubation-reduced osmium tetroxide. a) Portion of a centrilobular hepatocyte showing close packing of peroxisomes which are exclusively located within the SER-glycogen areas. Note the compartmentation of the cytoplasm: numerous mitochondria define the border between well-developed stacks of parallel RER—cisternae and the peroxisome-containing SER-glycogen areas. × 19,000. b) The closely apposed membranes within a peroxisome stack are flattened and separated by a uniform distance (arrowhead) which is consistently traversed by numerous fine filaments linking the outer membrane leaflets. × 123,000. c) The contact zone between the apposed peroxisomal membranes exhibits a considerable length and straight course. Note the matrical plates (arrowheads) which appear as curled densities in the peroxisomal matrix. × 55,000. d) Two large peroxisomal profiles are linked by a small, moderately stained organelle segment which is closely apposed and creates slight impressions upon their limiting membranes (small arrowhead). The large arrowhead demarcates the eccentrically located crystalline nucleoid. × 58,000. Bars, (a) 1 μm, (b) 100 nm, (c) (d) 250 nm.

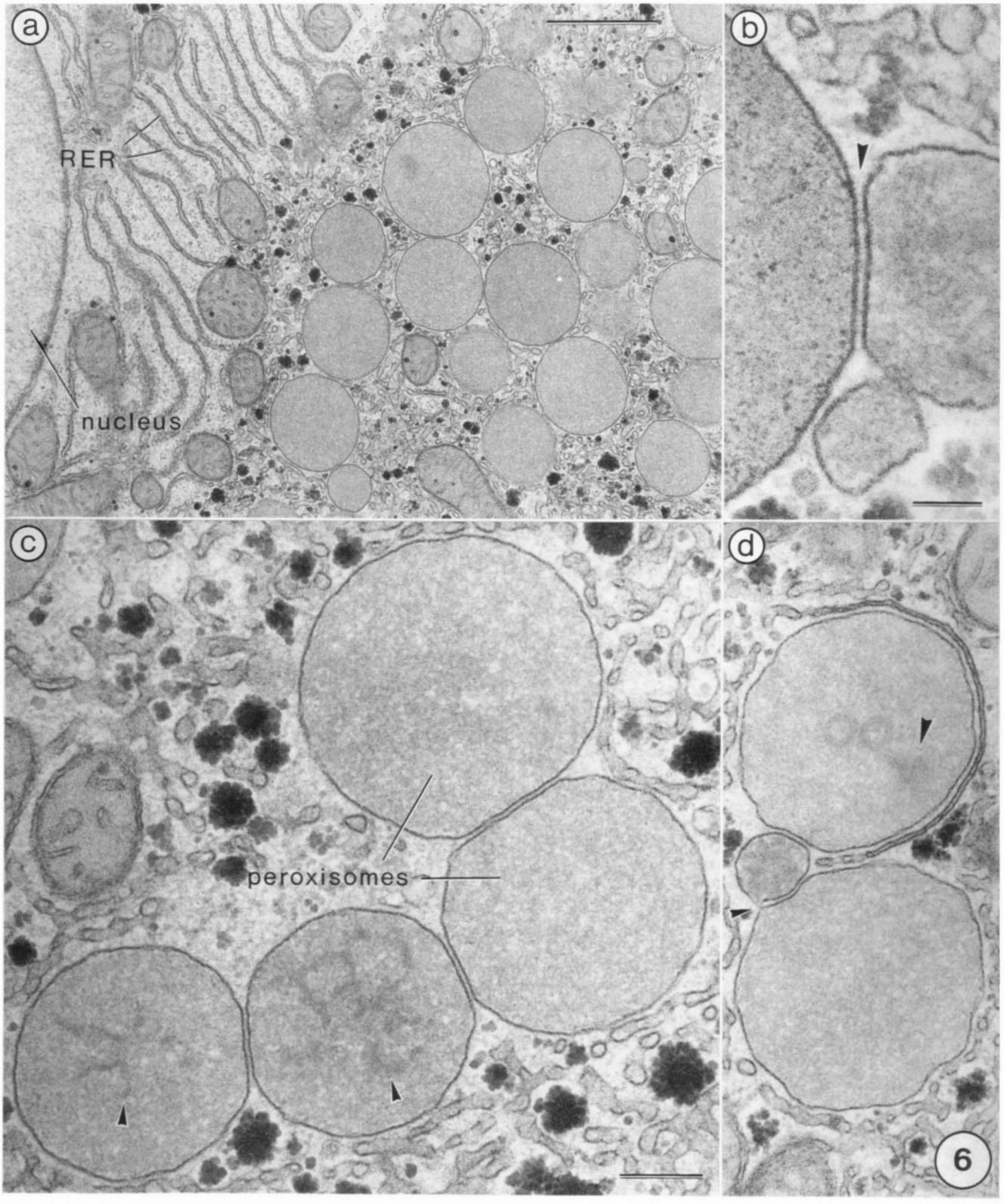

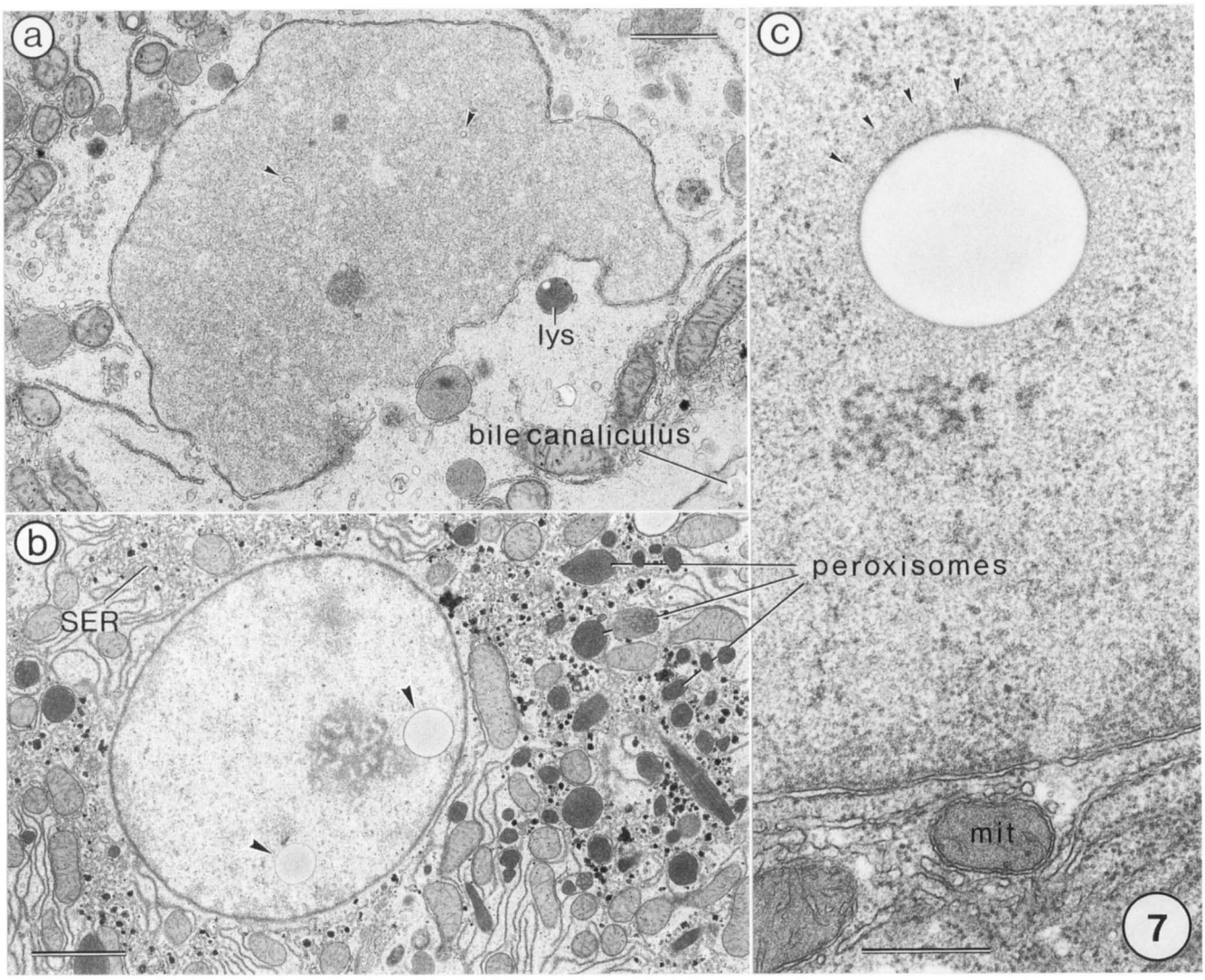

Fig. 7. Electron micrographs of hepatocytes of the midzonal region of the male rat liver treated for 2 weeks with gemfibrozil. a) During the late anaphase stage of mitosis the reconstitution of the nuclear envelope on the chromosome surface is clearly seen. Note the intranuclear membrane vesicles (arrowheads) and the close association of peroxisomes to the reassembling nuclear envelope. lys, lysosome. Short DAB-incubation-reduced osmium tetroxide. × 12,500. b) In random thin sections one or two intranuclear lipid inclusions (arrowheads) can be frequently demonstrated. SER, network of smooth endoplasmic reticulum. DAB-reduced osmium tetroxide. × 7,000. c) The intranuclear lipid droplets are surrounded by both an electron-dense leaflet and a concentric zone composed of a fine network of interconnected filaments (arrowheads). mit, mitochondrion. Short DAB-incubation-buffered osmium tetroxide. × 38,000. Bars, (a) 1 μm, (b) 2 μm, (c) 500 nm.

mental conditions known to cause proliferation of these organelles (12, 25, 29, 31). Among these compounds only aspirin seems to induce a high incidence of plate- containing peroxisomes (40). Recently, Furukawa and coworkers (40, 41) have demonstrated that matrical plates also occur in cultured rat hepatocytes obtained from carcinogen-induced preneoplastic lesions treated either with or without clofibrate. The data imply that the development of matrical plates is not necessarily associated with peroxisome proliferation and, furthermore, not specifically induced by peroxisome proliferators.

Peroxisome "stacking"

The data presented clearly demonstrate that gemfibrozil induces a specific packing or stacking pattern of peroxisomes in the form of rouleau- or chain-like structures which are most abundant and best developed in the inner midzonal and outer centrilobular regions of the liver lobule and less pronounced or absent during mitosis. Thus, peroxisome linking does not seem to be a random phenomenon but reflects a specific functional compartmentation of the organelle, particularly in nondividing

hepatocytes of the inner lobular regions. As compared to the marked effects produced by gemfibrozil, compounds such as clofibrate, nafenopin, or perfluorooctanoate only elicit minimal peroxisome packing in rat liver (data not shown).

The structural maintenance of peroxisome coupling seems to be established by filaments or cross-bridges within the intermembranous space linking different organelles and/or segments of the same organelle. In view of the fusion concept of peroxisomes, it is interesting to note that peroxisomal profiles are intimately attached to each other but do not seem to fuse. The observation of numerous pearl-like and tubular profiles extending from large organelles mostly located in the midzonal region assumes that chain-like peroxisome structures arise from individual pre-existing organelles by elongation, segmentation, and enlargement, thereby creating a dense peroxisomal network throughout the cytoplasm.

Striking peroxisome stacking and uniform organelle spacing have also been demonstrated in various lipid-synthesizing epithelia during increased lipid biosynthesis and initial lipid storage (for review see ref. 42). The current functional significance of peroxisome coupling with the concomitant development of enlarged tight membrane contact zones is to date unknown. Liver peroxisomes of gemfibrozil-treated rats offer a unique possibility to elucidate the cross-bridging mechanisms of intracellular membrane-to-membrane linkages.

Myelin-like bodies and fingerprint-whorls of smooth endoplasmic reticulum

The present study indicates that gemfibrozil induces a marked proliferation of smooth endoplasmic reticulum with the development of concentric myelin-like bodies and fingerprint-whorls which are easily recognizable by light microscopy. The lamellar structures are preferentially located adjacent to the nucleus and consist of either densely packed paired membranes or irregularly fenestrated cisternae. The greatest concentration of lamellar bodies is found in the lobular regions, whereas hepatocytes within the outer midzonal cell layers frequently contain both myelin-like bodies and fingerprint-whorls. Most recently, the assembly and formation of lamellar paired membrane stacks of SER have been reported to result in overproduction of 3-hydroxy-3-methylglutaryl-coenzyme A reductase in yeast strains and in Chinese hamster ovary-derived UT-1 cells as well as in rat hepatocytes. Using immunoelectron microscopy, the protein is clearly concentrated in the lamellar stacks surrounding the nucleus in yeast (43) and UT-1 cells (44) as well as in whorled SER in rat hepatocytes (45). However, myelin-like bodies and fingerprint-whorls have previously been described also in rat hepatocytes in response to a variety of drugs and toxins unrelated to cholesterol synthesis. Thus, the function of these whorled SER membrane aggregations and the significance of their distinct portal-central distribution after gemfibrozil exposure remain to be elucidated.

Nuclear lipid inclusions

Administration of hypolipidemic drugs, industrial plasticizers, and diverse chemicals to rodents results not only in a marked proliferation of peroxisomes and the smooth endoplasmic reticulum, but also in a periportal accumulation of fine lipid droplets (46–48). These findings are in agreement with our observations showing the identical distribution pattern of small lipid droplets in the rat liver lobule treated for 2 weeks with gemfibrozil. However, the concomitant occurrence of nuclear lipid inclusions, to our knowledge, has not yet been reported. Only one study describes nuclear lipid inclusions in the liver of two hyperlipoproteinemic patients under long-term gemfibrozil treatment, suggesting a positive correlation between specific drug treatment and nuclear alterations in humans as well (18).

The nuclear lipid droplets of treated rats are not derived from the cytoplasm by invagination of the nuclear envelope. They are surrounded by a thin electron-dense lipid leaflet and an adjacent filamentous zone which continuously extends into the nuclear matrix. Recently, we observed identical nuclear lipid droplets in the rat liver treated with perfluorooctanoate which belongs to the group of potent peroxisome proliferators (5). These agents, therefore, seem to trigger a common reaction pattern in the nuclear lipid/protein metabolism. To date, the origin, composition, and functional significance of these nuclear lipid droplets are unknown. The questions remain to be elucidated as to whether this results from de novo and excess nuclear lipid synthesis or more probably from increased lipid transfer from the cytoplasm.

This paper is dedicated to Professor Dr. Ortmann on the occasion of his 75th birthday. The authors thank Ms. I. Kuhn-Krause and Ms. U. Wald for their excellent technical assistance. We are grateful to Dr. Roger S. Newton (Warner-Lambert Company) for the initial supply of gemfibrozil. This study was supported by a grant of the Deutsche Forschungsgemeinschaft Go 432/1-1 to K. G. and by grant DK 32852 from the National Institutes of Health to S. K.
Manuscript received 10 May 1989 and in revised form 10 July 1989.

REFERENCES

1. Reddy, J. K., and N. D. Lalwani. 1983. Carcinogenesis by hepatic peroxisome proliferators: evaluation of the risk of hypolipidaemic drugs and industrial plasticizers to humans. *CRC Crit. Rev. Toxicol.* **12:** 1–58.
2. Hawkins, J. M., W. E. Jones, F. W. Bonner, and G. G. Gibson. 1987. The effect of peroxisomal proliferators on microso-

mal, peroxisomal, and mitochondrial enzyme activities in the liver and kidney. *Drug Metab. Rev.* **18:** 441–515.
3. Moody, D. E., and J. K. Reddy. 1976. Morphometric analysis of the ultrastructural changes in rat liver induced by the peroxisome proliferator SaH 42-348. *J. Cell Biol.* **71:** 768–780.
4. Baumgart, E., K. Stegmeier, F. H. Schmidt, and H. D. Fahimi. 1987. Proliferation of peroxisomes in pericentral hepatocytes of rat liver after administration of a new hypocholesterolemic agent (BM 15766). *Lab. Invest.* **56:** 554–564.
5. Just, W., K. Gorgas, F-U. Hartl, P. Heinemann, M. Salzer, and H. Schimassek. 1989. Biochemical effects and zonal heterogeneity of peroxisome proliferation induced by perfluorocarboxylic acids in rat liver. *Hepatology.* **9:** 570–581.
6. Fukuda, K., H. Shindo, S. Yamashina, and V. Mizuhira. 1978. Fine structural changes in the hepatic microbodies of rats treated with hypolipidemic agents gemfibrozil and clofibrate. *Acta Histochem. Cytochem.* **11:** 432–442.
7. Gray, R. H., and F. A. de la Iglesia. 1984. Quantitative microscopy comparison of peroxisome proliferation by the lipid-regulating agent gemfibrozil in several species. *Hepatology.* **4:** 520–530.
8. Karnovsky, M. J. 1971. Use of ferrocyanide-reduced osmium tetroxide in electron microscopy. *J. Cell Biol.* **51:** 284 abstr.
9. Richardson, K. C., L. Jarett, and E. H. Finke. 1960. Embedding in epoxy resins for ultrathin sectioning in electron microscopy. *Stain Technol.* **35:** 313–325.
10. Reynolds, E. S. 1963. The use of lead citrate at high pH as an electron opaque stain in electron microscopy. *J. Cell Biol.* **17:** 208–229.
11. LeHir, M., V. Herzog, and H. D. Fahimi. 1979. Cytochemical detection of catalase with 3,3'-diaminobenzidine. A quantitative reinvestigation of the optimal conditions. *Histochemistry.* **64:** 51–66.
12. Hruban, Z., M. Gotoh, A. Slesers, and S-F. Chou. 1974. Structure of hepatic microbodies in rats treated with acetylsalicylic, clofibrate, and dimethrin. *Lab. Invest.* **30:** 64–75.
13. Cohen, A. J., and P. Grasso. 1981. Review of the hepatic response to hypolipidaemic drugs in rodents and assessment of its toxicological significance to man. *Food Cosmet. Toxicol.* **19:** 585–605.
14. Todd, P. A., and A. Ward. 1988. Gemfibrozil. A review of its pharmacodynamic and pharmacokinetic properties, and therapeutic use in dyslipidaemia. *Drugs.* **36:** 314–339.
15. Burger, P. C., and F. B. Herdson. 1966. Phenobarbital-induced fine structural changes in rat liver. *Am. J. Pathol.* **48:** 793–819.
16. Loud, A. V. 1968. A quantitative stereological description of the ultrastructure of normal rat liver parenchymal cells. *J. Cell Biol.* **37:** 27–46.
17. de la Iglesia, F. A., S. M. Pinn, J. Lucas, and E. J. McGuire. 1981. Quantitative stereology of peroxisomes in hepatocytes from hyperlipoproteinemic patients receiving gemfibrozil. *Micron.* **12:** 97–98.
18. de la Iglesia, F. A., J. E. Lewis, R. A. Buchanan, E. L. Marcus, and G. McMahon. 1982. Light and electron microscopy of liver in hyperlipoproteinemic patients under long-term gemfibrozil treatment. *Atherosclerosis.* **43:** 19–37.
19. Hanefeld, M., C. Kemmer, W. Leonhardt, K. D. Kunze, W. Jaross, and H. Haller. 1980. Effects of *p*-chlorophenoxyisobutyric acid (CPIB) on the human liver. *Atherosclerosis.* **36:** 159–172.
20. Hanefeld, M., C. Kemmer, and E. Kadner. 1983. Relationship between morphological changes and lipid-lowering action of *p*-chlorophenoxyisobutyric acid (CPIB) on hepatic mitochondria and peroxisomes in man. *Atherosclerosis.* **46:** 239–246.
21. Frick, M. H., O. Elo, K. Haapa, O. P. Heinonen, P. Heinsalmi, P. Helo, J. K. Huttunen, P. Kaitaniemi, P. Koskinen, V. Manninen, H. Mäenpää, M. Mälkönen, M. Mänttäri, S. Norola, A. Pasternack, J. Pikkarainen, M. Romo, T. Sjöblom, and E. A. Nikkilä. 1987. Helsinki Heart Study: primary-prevention trial with gemfibrozil in middle-aged men with dyslipidemia. Safety of treatment, changes in risk factors, and incidence of coronary heart disease. *N. Engl. J. Med.* **317:** 1237–1245.
22. Bendayan, M., and J. K. Reddy. 1982. Immunocytochemical localization of catalase and heat-labile enoyl-CoA hydratase in the liver of normal and peroxisome proliferator-treated rats. *Lab. Invest.* **47:** 364–369.
23. Rao, M. S., and J. K. Reddy. 1987. Peroxisome proliferation and hepatocarcinogenesis. *Carcinogenesis.* **8:** 631–636.
24. Reddy, J. K., J. R. Warren, M. K. Reddy, and N. D. Lalwani. 1982. Hepatic and renal effects of peroxisome proliferators: biological implications. *Ann. N. Y. Acad. Sci.* **386:** 81–110.
25. Gotoh, M., C. Griffin, and Z. Hruban. 1975. Effect of citrate and aminotriazole on matrical plates induced in hepatic microbodies. *Virchows Arch. B Cell Pathol.* **17:** 279–294.
26. Yarrington, J. T., D. J. Sprinkle, D. E. Loudy, T. Kariya, and J. P. Gibson. 1981. Effect of the hypolipidemic drug RMI 14,514 on hepatic ultrastructure of rats. *Exp. Mol. Pathol.* **34:** 307–322.
27. Reddy, J., and D. Svoboda. 1973. Microbody (peroxisome) matrix: transformation into tubular structures. *Virchows Arch. Abt. B Zellpathol.* **14:** 83–92.
28. Fahimi, H. D., A. Reinicke, M. Sujatta, S. Yokota, and M. Özel. 1982. The short- and long-term effects of bezafibrate in the rat. *Ann. N. Y. Acad. Sci.* **386:** 111–133.
29. Tsukada, H., Y. Mochizuki, and M. Gotoh. 1975. Matrical inclusions induced by clofibrate in hepatic microbodies of rats fed 2-acetylaminofluorene. *J. Natl. Cancer Inst.* **54:** 519–523.
30. Tsukada, H., Y. Mochizuki, and M. Gotoh. 1978. Alterations in peroxisomes of hepatomas. *Adv. Exp. Med. Biol.* **92:** 331–380.
31. Gotoh, M., Y. Mochizuki, N. Sawada, and H. Tsukada. 1982. Matrical inclusions of peroxisomes induced by clofibrate in preneoplastic hepatocytes of rats fed 3'-methyl-4-dimethylaminoazobenzene. *Gann.* **73:** 7–13.
32. Mochizuki, Y., and K. Furukawa. 1984. The formation of matrical tubules in peroxisomes by aspirin in hyperplastic liver nodules of rats induced by 2-acetylaminofluorene. *Tumor Res.* **19:** 31–38.
33. Dalton, H. J. 1964. An electron microscopic study of a series of chemically induced hepatomas. *In* Cellular Mechanisms and Cancer. P. Emmelot, and O. Mühlbock, editors. Elsevier, Amsterdam. 211–225.
34. Dalton, A. J. 1965. Correlation between rate of growth and fine structure of hepatomas from rats. *In* Primary Hepatomas. W. J. Burdette, editor. University of Utah Press, Salt Lake City. 51–64.
35. Langer, K. H. 1968. Feinstrukturen der Mikrokörper (Microbodies) des proximalen Nierentubulus. *Z. Zellforsch.* **90:** 432–446.
36. Barrett, J. M., and P. M. Heidger, Jr. 1975. Microbodies of the rat renal proximal tubules: ultrastructural and cytochemical investigations. *Cell Tissue Res.* **157:** 283–305.
37. Kalmbach, P., and H. D. Fahimi. 1978. Peroxisomes: identification in freeze-etch preparations of rat kidney. *Cell Biol. Int. Rep.* **2:** 389–396.
38. Yokota, S., A. Völkl, T. Hashimoto, and H. D. Fahimi. 1987. Immunoelectron microscopy of peroxisomal enzymes: their substructural association and compartmentalization in rat kidney peroxisomes. *In* Peroxisomes in Biology and Medicine.

H. D. Fahimi, and H. Sies, editors. Springer, Heidelberg-New York. 116–127.

39. Angermüller, S., and H. D. Fahimi. 1988. Heterogeneous staining of D-amino acid oxidase in peroxisomes of rat liver and kidney. A light and electron microscopic study. *Histochemistry.* **88:** 277–285.
40. Furukawa, K., Y. Mochizuki, N. Sawada, M. Gotoh, and H. Tsukada. 1988. Morphometric and cytochemical evaluation of clofibrate-induced peroxisomal proliferation in adult rat hepatocytes cultured on floating collagen gels. *Virchows Arch. B. Cell Pathol.* **55:** 279–285.
41. Furukawa, K., and Y. Mochizuki. 1986. Formation of abnormal inclusions in peroxisomes of cultured hepatocytes of hyperplastic nodules in the rat by 2-acetylaminofluorene. *Proc. XIth Int. Congr. Electron Microsc.* **3:** 2587–2588.
42. Gorgas, K. 1987. Morphogenesis of peroxisomes in lipid-synthesizing epithelia. *In* Peroxisomes in Biology and Medicine. H. D. Fahimi, and H. Sies, editors. Springer, Heidelberg-New York. 1–17.
43. Wright, R., M. Basson, L. D'Ari, and J. Rine. 1988. Increased amounts of HMG-CoA reductase induce "karmellae": a proliferation of stacked membrane pairs surrounding the yeast nucleus. *J. Cell Biol.* **107:** 101–114.
44. Pathak, R. K., K. L. Luskey, and R. G. W. Anderson. 1986. Biogenesis of the crystalloid endoplasmic reticulum in UT-1 cells: evidence that newly formed endoplasmic reticulum emerges from the nuclear envelope. *J. Cell Biol.* **102:** 2158–2168.
45. Singer, I. I., S. Scott, D. M. Kazazis, and J. W. Huff. 1988. Lovastatin, an inhibitor of cholesterol synthesis, induces hydroxy-methylglutaryl-coenzyme A reductase directly on membranes of expanded endoplasmic reticulum in rat hepatocytes. *Proc. Natl. Acad. Sci. USA.* **85:** 5264–5268.
46. Mann, A. H., S. C. Price, F. E. Mitchell, P. Grasso, R. H. Hinton, and J. W. Bridges. 1985. Comparison of the short-term effects of di(2-ethylhexyl) phthalate, di(n-hexyl) phthalate, and di(n-octyl) phthalate in rats. *Toxicol. Appl. Pharmacol.* **77:** 116–132.
47. Elcombe, C., M. S. Rose, and I. S. Pratt. 1985. Biochemical, histological, and ultrastructural changes in rat and mouse liver following the administration of trichloroethylene: possible relevance to species differences in hepatocarcinogenicity. *Toxicol. Appl. Pharmacol.* **79:** 363–376.
48. Price, S. C., R. H. Hinton, F. E. Mitchell, D. E. Hall, P. Grasso, G. F. Blane, and J. W. Bridges. 1986. Time and dose study on the response of rats to the hypolipidaemic drug fenofibrate. *Toxicology.* **41:** 169–191.